USING NMT PRINCIPLES IN PREDICTING PERFORMANCE OF A POWERHOUSE IN THE HIMALAYAS, INDIA

Panayiotis Chryssanthakis, Rajinder Bhasin, Nick Barton
Rock Engineering Department

Norwegian Geotechnical Institute,
Postboks 3930 Ullevaal Hageby, N-0806 OSLO Norway

SYNOPSIS

This paper describes some of the NMT (Norwegian Method of Tunnelling) priciples applied to an underground powerhouse in the Himalayas. The discontinuum code UDEC-BB (Barton - Bandis joint constitutive model) has been used for two-dimensional modelling of the Nathpa Jhakri powerhouse in low strength anisotropic rocks in the Himalayas region in India. The powerhouse has a 20 m span, 49 m high walls and is 216 m in length. The main rocks in the area are metamorphic rocks such as gneisses, schists, gneissose schists and basic intrusives (amphibolites). The low strength metamorphosed rocks are quartz mica schists, biotite schists, and muscovite schists. The input data required for UDEC-BB have been derived from Q-system logging, from index testing density, porosity, specific gravity, uniaxial compressive tests and rock joint characterization of drill core (JRC, JCS, ϕ_r) and from in situ stress measurements, using hydrofracturing and overcoring techniques and from sonic wave measurements. The stabilizing effect of the fiber reinforced shotcrete S(fr) in underground constuctions is now possible to model in UDEC-BB. With the new version 2.02 of UDEC - BB (December '95) it is possible to model both the effect of applying S (fr) and the rock reinforcement bolts that are installed afterwards. In this paper we present results from numerical modelling for modelled S (fr) thickness varying between 15 cm for the arch and 10 cm for the walls (model 1) and 25 cm for the arch and 20 cm for the walls (model 2). In addition to this, we also modell the Q-system derived rock bolt pattern of 32 mm in diameter with alternating length 6 and 12 m bolt at 3 m spacing. By the time of writing this article (December '95) the excavation of the powerhouse was almost completed. The results of this most recent modelling work are discussed. A maximum deformation value of approximately 45 mm on the cavern walls is predicted after the final excavation of the powerhouse. The maximum recorded deformation on powerhouse arch by the time of writing this article was 24 mm. There are strong indications that the deformation on the cavern walls may be around 40 mm.

1 INTRODUCTION

In recent years construction of tunnels through low strength anisotropic rocks such as phyllites, shales and schists in the Himalayan Regions has generated new thoughts in anticipating and assessing the problems in such rocks. The problems faced in tunnelling through these rocks include squeezing ground if the rock contains a considerable amount of clay minerals and loosening of the rock mass in the case of layered and jointed rock masses. Loosening results in the separation of the rock mass from the main body which produces a dead load.
The behaviour of low strength anisotropic rocks cannot easily be assessed through common engineering experience due to the variation of mineral assemblage, fabric and geo-mechanical properties. Hence, a detailed engineering geological assessment of such rocks is warranted.

In this paper the three types of schists namely, quartz mica schist, biotite schist and muscovite schist encountered in the head race tunnel and in the underground powerhouse at the project site have been analyzed and have also been modelled numerically with weak zones in the jointed rock mass (Figure 1). The index studies carried out include petrographic and petrofabric analysis through electron microscopy, thin sections and X-ray diffraction. The geo-mechanical properties have been evaluated with emphasis on their behaviour in underground structures.

Two approaches have been adopted to study the geo-mechanical properties of these rock masses. The first approach includes laboratory tests to find the index properties of the rock which include the density, specific gravity, porosity, sonic wave velocity and the uniaxial compressive strength of the rock samples. The second approach estimates the strength and deformability of a jointed rock mass through the recently updated Q-System of rock mass classification (Grimstad & Barton, 1993). In-situ rock stress measurements for finding the principal stress directions have also been carried out. The numerical modelling techniques (UDEC) i.e., the distinct element code (Cundall, 1980) which incorporates the strength and deformability properties of the joints and intact rock separetely, has been used to predict the

behaviour of the rock mass. With the new version 2.02 of UDEC - BB (Dec''95) it is possible to model both the fiber reinforced shotcrete and the actual rock bolts that are installed after the S (fr). The modelled thickness of the S(fr) varied between 15 cm for the arch and 10 cm for the walls while the rock bolt pattern (bolts of 32 mm diameter) used for the crown and the walls of the powerhouse had a spacing of 3 m with alternating length of 6m and 12m.

2 BRIEF GEOLOGICAL DESCRIPTION OF THE SITE

The Nathpa Jhakri Hydroelectric Project is located between 77°-78° longitude and 31°-32°N latitude on the snow fed Satluj river in the Kinnaur and Simla district of Himachal Pradesh in the Himalayan Region of India .
The rocks in the area are metamorphic rocks such as gneisses, schists, gneissose schists and basic intrusives (amphibolites), granite and pegmatites. These Pre-Cambrian rocks belong to the Wangtu Jeori Gneissic Complex in the eastern margin of the Rampur Window (Thakur, 1992). The metamorphism in these rocks is essentially of a regional type over an extensive area where intensive folding under pressure has converted the texture into schistose or gneissose. The schists are intruded by quartz veins of varying thicknesses and boudins have been formed due to metamorphic sweating. The gneissose schists and schists of the area are foliated with an East-West strike and dip 35° with some local variation in the northerly direction.

More than five joint sets have been recorded in the project area but rarely more than three joint sets plus random are encountered at any location. At places gouge seams are also associated with some of the joints, especially the foliation joints. The rock cover above the tunnel grade usually varies from 200-600m and for small stretches the rock cover exceeds 1000m.

The area encompassing the powerhouse site contains essentially quartz-mica schist, patches of biotite schist and muscovite (sericite) schist. These are moderately to closely jointed rocks and at places slightly to moderately weathered (ISRM, 1981). The rocks are intruded by quartz veins of varying thicknesses often forming boudins which follow the foliation trend. The quartz mica schist is affected by small scale crenulation folds which are mainly the expressions of the changes in mineralogy and fabric that were required to accommodate distortion of the rock body. This makes the rock mass stronger than it would have been with planar foliation, because sliding is not likely to occur along the folded foliation planes, unless the fold axis is parallel to the potential sliding direction.

3 ROCK MASS CLASSIFICATION

Rock mass classification systems provide guidelines for the estimation of support pressure and for the design of tunnel reinforcement. The Q-System of Barton et al., 1974, developed at the Norwegian Geotechnical Institute (NGI), has been applied extensively to derive the geotechnical parameters needed for predicting the performance of the rock mass. The alignment of the powerhouse cavern was selected taking into consideration the strike direction of the major discontinuity planes. The E-W striking foliation joints constitute the major discontinuities, suggesting a N-S alignment for the powerhouse axis in order to avoid wall stability problems. The orientation of the major principal stress σ_H was parallel to the long axis of the powerhouse cavern (N-S), which would not be the most favourable if major jointing also trended parallel to σ_H. Fortunately this is not the case here. Rock mass classification, based on core characterization, in the powerhouse drift indicated Q values in the range of 0.15 - 10.

Detailed engineering geological mapping of the rock and rock joints has been carried out. The same geotechnical logging chart use in this project has being used extensively as an aid in data collection and presentation for the design of underground caverns for radioactive wastes in England (Barton et al., 1992) and for the mapping of large underground openings (Bhasin et al., 1993 and Bhasin, 1994). The Q value was estimated for stretches of 10m in length. The Q values mapped in the pilot tunnel in the cavern range from 0.73 to 32 with the weighted average being 2.7. This number is derived as follows:

$$Q = \frac{69.5}{5.2} x \frac{2.6}{2.6} x \frac{0.958}{4.9} = 2.7$$

This reflects a rather poor rock quality requiring support after each excavation step (pilot heading, slashing of walls & benching) so that the redistributed stresses in the underground opening do not exceed the low strength of the rock and cause excessive deformations. Detailed joint surveys in the excavated portions of the cavern provided data on joint orientations, joint character and spacing. Measurement of strike and dip of the main discontinuities were made throughout the pilot heading. Although the joint pattern is quite irregular, three sets of joints have been identified. Set 1 is

the foliation joint striking generally in the E-W direction across the long axis of the cavern with a dip of 35° towards N. Sets 2 and 3 are striking approximately in the NS direction dipping steeply (70-90°) in the E and W directions respectively. The foliation joints are mostly persistent with lengths varying from 5-20m. Joint set 1 is considered as the most unfavourable for the stability of the cavern due to its persistence and association with gouge seams. Set 2 or Set 3 depend on the development and persistence of these joint sets in different areas of the pilot heading. Some thin shear zones of 10-20cm thick also follow the foliation trend. A majority of the joints are healed with quartz mineralization. This has often resulted in a higher JCS (Joint wall compressive strength) value obtained through Schmidt hammer readings in comparison to the unconfined compressive strength of the rock (σ_c). Values of other key geotechnical parameters such as joint frequency F (per meter), joint spacing S (m), joint roughness coefficient JRC, Permeability K (m/s), major principal stress (σ_1; horizontal and along the long axis of the cavern), joint volumetric count J_v (per m^3) and joint roughness amplitude measurements (a/L) are also registered.

4 ROCK STRESS MEASUREMENTS

Rock stress measurements using both the hydraulic fracturing and the overcoring techniques were carried out in the powerhouse drift by The Central Soil and Material Research Station (CSMRS), New Delhi. Three EX size (38mm) boreholes (2 horizontal & 1 vertical) striking NS, EW and in the vertically upwards direction were drilled in the NS oriented drift. A total of 21 hydraulic fracturing tests were performed in the selected test sections of the three boreholes. The depth of testing below surface ranged from 250-300m and the results indicate the following:

Maximum horizontal stress (σ_1) = 7.14 MPa in N 30° E direction
Minimum horizontal stress (σ_3) = 3.93 MPa in N 60° W direction
Vertical stress (σ_2) = 5.89 MPa

Since two of the holes are in a horizontal direction, the principal stresses perpendicular to the holes (i.e., one vertical and the other horizontal) are determined. In the case of a vertical borehole the principal stresses determined are both horizontal. The calculated vertical stress is in close agreement with the estimated vertical stress of 6.6 MPa obtained through the weight of the overlying rock (depth 250m, density 2.7 g/cm^3). Tests using the overcoring technique have given higher values of stresses than those obtained through hydraulic fracturing. For these anisotropic rocks the rock stresses obtained through hydraulic fracturing test are consi- dered appropriate for numerical simulation purposes.

5 BRIEF DESCRIPTION OF THE FIBER REINFORCED SHOTCRETE SUBROUTINE IN UDEC-BB

The numerical code used at NGI, version 2.02 (UDEC-BB with S (fr)) is a version of Cundall's distinct element two-dimensional code (Cundall 1980). Application of this code in earlier projects can be found in (Makurat et.al. 1990), (Barton et al. 1992). The main characteristics of the fibre reinforced subroutine in UDEC are as follows:

- Possibility to apply S(fr) not only on idealized (circular) tunnel peripheries but also in uneven peripheries.
- Possibility to model the variation in adhesion between the S(fr) and rock interface (e.g difference in schist and granite).
- Possibility to model the ductile behaviour of S(fr) after failure.
- Possibility to model the bolt reinforcement piercing the S(fr). The last feature has a limitation since the S(fr) and bolts are fixed in one single point only.

Six different types of graphs can be produced in connection with the S (fr) subroutine in UDEC-BB. These different types of graphs are :

a. Axial forces on the S (fr) structure
b. Shear forces on the S (fr) structure.
c. Moments on the S (fr) structure
d. Axial forces on the S (fr)/Rock interface
e. Shear forces on the S (fr)/Rock interface
g. Failure plot of the S (fr) (structural elements)

Note that all force values refer to MegaNewtons(MN). The conversion is 0.01 MN = 1 tonne (force). The area of application of the forces is 1m (depth of model) x 0.1 m (e.g for S (fr) thickness) = 0.1 m^2 . The necessary UDEC parameters for modelling the S (fr) and their values used in this modelling work are listed in Table 2:

6 DESCRIPTION OF THE NUMERICAL MODELS

In order to get a better understanding of the performance of this underground structure, two numerical models were run and compared. The analysis of the results in this paper is mainly focusing on the behaviour of the S (fr) and the rock bolts. Both models have exactly the same joint geometry, (Figure 1), intact rock, joint properties, boundary conditions and in-situ rock stresses. The original joint geometry in Figure 1 also contain the transformer hall area which will be excavated and reported in a later stage. The difference between the numerical models are:

- The 1st model (Model 1) has S (fr) thickness of 15 cm applied on the arch and 10 cm on the walls.
- The 2nd model (Model 2) has a S (fr) thickness of 25 cm applied on the arch and 20 cm on the walls.

The powerhouse has been excavated in three stages (Figure 1). The numbers in the cavern area refer to the excavation steps used in the numerical simulation. The rock bolt pattern (bolts of 32 mm diameter) that is used in the crown and the walls of the powerhouse was also modelled numerically (bolt spacing 3.0 m length 6m and 12m). The rock bolt pattern is shown in Figure 2.

7 INPUT PARAMETERS FOR NUMERICAL MODELLING

The rock mass deformation modulus E is estimated from the following Q-System relation (Barton, 1983), where Q=2.7 The Poisson's ratio was estimated to 0.25.

$$E_{mean} = 25 \log_{10} Q = 10.78 \text{ GPa}$$

7.1. Shear strength parameters for the joints

The number of joints in the model is reduced compared to reality and the easterly and westerly dipping joint lengths are excessive (longer) for all but the most persistent joints. An inevitable approximation of 2D modelling is that the joints perpendicular to the tunnel axis cannot be represented by the dip while the joints striking parallel to the tunnel axis are representable with dip. Joint roughness profiles were measured during the rock core characterization along 100mm or longer joint surfaces in the existing rock caverns.

The three joint sets and the shear zones existing in the powerhouse area have been modelled. The input parameters for the non-linear joint model (Barton and Bandis, 1990) were used for the three joint sets while Mohr - Coulomb properties were used for the behaviour of the shear zones. The input data for rock joints properties are shown in Table 1.

Joint set 1 is the foliation joint striking in the E - W direction across the long axis of the cavern with a dip of 35 degrees towards the north. Joint sets 2 and 3 are striking approximately in the N- S direction dipping steeply (70 -90) degrees in the E and W directions respectively. The shear zones are marked by thicker lines on the joint geometry plot (see Figure 1). The modelled shear zones had a cohesion (c) = 400 kPa and a friction angle (ϕ) of 16 degrees.

7.2 . Excavation stages and reinforcement

The rock mass in the cavern arch and the walls were numerically reinforced by untensioned fully grouted rock bolts and anchors after each numerical excavation step. The rock bolt pattern, which forms a part of the input data for the powerhouse cavern, has been derived from the analysis of both the original and updated Q-System (Grimstad & Barton, 1993). It consists of 32mm dia., 6 and 12m long bolts placed alternatively at 3m
c/c spacing. The bolt yield strength was estimated to 41 tnf. Varying S (fr) thickness between 10 and 25 cm was sprayed on the arch and the walls to be followed by the bolt installation. Each of the excavation steps was first run to equilibrium without any use of reinforcement. When 100 % of deformation was achieved the point where approximately 50 % of deformation, had occured was then back tracked. The fiber reinforced shotcrete was then applied, the rock mass was then left to deform further (about 70% of the total expected) and then the installation of the bolts followed. This was done in an attempt to allow for the elastic deformation that will have already occured before the S (fr) and bolts were installed. The modelled properties of the fiber reinforced shotcrete are shown in Table 2.

Table 1. Jointed rock properties for the foliation joints and joint sets 2 & 3.

Parameter	Joint set 1 foliation joints	Joint set 2 & Joint set 3
JRC_0 (Joint Roughness Coefficient)	10	11
JCS_0 MPa (Joint Compressive Strength)	37.85	37.85
ϕ_r degrees ° (Residual friction angle)	25	26
σ_c MPa (Uniaxial Compressive strength of intact rock)	35	35
L_0 m (Laboratory scale joint length)	0.1	0.1
L_n m (Assumed conservative block dimension)	1.0	1.0
Aper mm (Initial joint mechanical aperture at zero load)	0.170	0.190

o

Table 2. Fiber reinforced shotcrete parameters used in the modelling work:

Parameter	Notation, units	Model 1	Model 2
Modulus of elasticity	E (MPa)	15	15
Poisson's ratio	ν	0.15	0.15
Density	D (kg/m^3)	2.5e3	2.5e3
Compressive yield strength	Ycomp (MPa)	30	30
Tensile yield strength	Yield (MPa)	3	3
Residual tensile yield strength	Yresid	2	2
Thickness arch Thickness wall	Thick (m)	0.15 0.10	0.25 0.20
Number of sprayed points	NP	100 per section	100 per section
Angle of spraying	Theta (degrees)	varying	varying
Offset angle for spraying	Fa (degrees)	varying	varying
Interface friction in S(fr)/rock	Jfric (degrees)	60	60
Interface cohesion in S(fr)/rock	Jcoh (MPa)	0.5	0.5
Interface tension (bond) in S(fr) / rock	Jtens (MPa)	0.86	0.86

8 NUMERICAL RESULTS - UDEC-BB, PREDICTION PERFORMANCE

8.1. Development of principal stress during excavation

The UDEC-BB results for each of the excavated steps are given in Table 3. The redistribution of stresses that occurred between the 1st and 3rd excavation steps is shown in Figure 3. The effect of high tangential stresses, more than 24 MPa, combined with the low compressive strength of the rock indicates spalling of blocks. The
area affected will be secured in practice through systematic rock bolting. In fact, spalling has been observed in the pilot tunnel of the powerhouse near the arch, consistent with the stress measurements (Grimstad and Barton, 1995). In the walls of the cavern some nearly stress free blocks can be observed. These blocks will be
secured in practice by the systematic rock bolting, S(fr) which was modelled in both models will effectively secure smaller blocks representing the detailed joint structure in the real case.

8.2 Development of deformation vectors during excavation

As expected there is a progressive development of deformation after the succesive excavation stages (see Table 4). The maximum deformation vector value is occurring on the walls of the cavern.. On the crown of the cavern the maximum numerical deformation recorded after the 3rd excavation step is 34 mm. Figure 4 shows the deformation vectors after the end of 1st and 3th excavation step. A magnification of the block deformations by 100 times is shown on the same Figure. It is obvious from this figure that cavern walls are subjected to relatively high deformations and need to be properly secured. The magnitude and the shape of the cavern walls indicate that the application of S(fr) on the walls will have little or no effect on the overall stability of the powerhouse. The applied S (fr) is expected to fail in tension at a rather early stage.

Table 3. Summary of the numerical results for model 1 and 2

Parameter	Model 1			Model 2		
	step 1	step 2	step 3	step 1	step 2	step 3
Maximum principal stress MPa	24.0	25.6	25.1	24.1	25.5	25.1
Maximum displacement (mm)						
arch crown	16.5	24.2	34.5	16.3	18.5	34.1
walls	-	27.4	46.2	-	27.3	45.0
Maximum shear displacement (mm)	11.5	17.2	24.9	11.4	16.04	24.6
Maximum axial forces on bolts (tnf)	22.1	22.4	27.1	22.3	25.86	27.3
Maximum axial forces on S (fr) (tnf)	233.0	214.6	130.9	348.8	84.5	3.2
Maximum moment on S (fr) (tnf)x m	2.8	3.7	2.5	9.7	2.6	2.2
Maximum shear forces on S (fr) (tnf)	9.9	14.9	6.2	33.6	5.4	1.7
Maximum normal forces on S (fr)/rock (tnf)	40.8	37.3	2.1	70.3	10.9	2.5
Maximum shear forces on S (fr)/rock (tnf)	69.3	66.5	36.1	120.7	46.1	4.4

8.3 Axial forces on bolts

According to these conservative two-dimensional analyses, the maximum axial forces on bolts are exceeding the 27.3 tnf yield limit after the 3rd excavation step. The yield limit in the bolts is derived from the 41 tnf yield limit for the 32 mm bolts times the reduction factor of 0.67 for the UDEC model of 1 m thickness. These are mainly bolts on the left hand side of the arch. It is interesting to note the development of bolt forces in the model with different thickness in S (fr) after the 3rd excavation step. It is obvious that the application of 20 cm of S (fr) instead of 10 cm contributes to a better distribution of the bolt forces in the rock mass. The bolt yield limit is reached in some locations on the arch of the powerhouse while on the walls the rock bolts are loaded considerably less.

8.4 Forces and moments on the S (fr), failure mode

Due to space limitations, the plots presented here are the axial and shear forces on the S (fr) after the 3rd excavation step for model 1 and 2 (see Figure 6 and 7). There is a substantial difference between the plots of Figure 6. The numbers in the plot refer to S (fr) on each location.There are three orders of magnitude difference between the axial stresses attained in the arch of the cavern and the axial stresses attained in the walls in model 1. This is because the thin S (fr), of 10 cm on the walls is broken in several areas as it can be seen in Figure 8 and is not able to attain significant stresses. On the contrary Model 2 with a thicker S (fr) of 20 cm is able to attain higher axial stresses on the walls and the arch sides. The same tendency is also observed on Figure 7 where the shear forces on the S (fr) are shown. Model 2 is able to attain higher shear forces on the cavern walls.
The areas were the S (fr) has failed are shown on Figure 8. It is interesting to observe that both models experience a compression failure on the arch of the cavern (see encircled area on Figure 8). Tension failure on the walls of the cavern is shown on the same Figure. The failure in tension of S (fr) in the walls of Model 2 is more intense than in Model 1. This is due to the fact that the thicker S (fr) in model 2 is attaining higher stresses than Model 1 while the tension failure limit in terms of stress (but not force) is the same in both models.

9 COMPARISON OF UDEC-BB RESULTS WITH MONITORED IN SITU RESULTS.

By the time of writing this paper, (December '95) the construction of the powerhouse had almost finished. The lower bench of the powerhouse is being excavated. The powerhouse construction had started with a 7 x 7 x 216m pilot tunnel adjacent to the pilot drift. Multiple point borehole extensometers (MPBX) have been installed in the roof of the pilot tunnel for monitoring the deformation of the rock. The maximum deformation on the arch of the powerhouse has been measured to about 24 mm. This value is not expected to increase dramatically when the powerhouse excavation is terminated.

The ongoing rock deformation monitoring programme, indicate that wall deformations have exceeded 24 mm (the maximum arch deformation) and will probably approach the maximum predicted value from the numerical models which is about 45 mm. The predicted numerical results will then be compared in detail with the measured performance of the cavern through the ongoing rock deformation monitoring programme. The results of such a comparison will be the subject of a future paper.

10 CONCLUSIONS

- Design and construction of a large span cavern with very high walls in low strength anisotropic rocks has been carried out at the site of a major hydroelectric power project in the Himalayan Region of India. The rock quality varies betwen poor, fair to good quality. The geo-mechanical properties of these rocks have been carefully assessed based on laboratory and field investigations for input to numerical modelling studies The rock mass characterization approach (Q-system) has been applied extensively to predict and evaluate appropriate rock reinforcement requirements for the underground caverns. The Q-values measured ranged between 0.7 and 32. The initial design was based on a mean Q-value of about 2.7.

- The input data for the UDEC-BB models have been derived from rock joint and rock mass characterization, cross-hole seismic tomography and rock stress measurments. The two numerical models that are presented in this article were similar, with variations mainly in the S (fr) thickness. Both models have also been numerically reinforced by systematic bolting. The bolt properties and bolt pattern have been checked by means of the Q-system. The discontinuum code UDEC-BB (Barton - Bandis joint constitutive model) has been used for the two-dimensional modelling of the Nathpa Jhakri powerhouse. This is a rather conservative approach since several features of the in situ rock behaviour cannot be modelled in 2 D (e.g the joints parrallel to the powerhouse axis have not been represented etc.). The potential shortcomings and the source of errors in this case are difficult to estimate. However, the presence of additional joint sets not parallel to the excavation tends to increase the deformation in practice, thus making a 2D approximation less conservative than usually assumed. Three dimensional modelling using the code 3DEC could have been an attractive alternative but due to time and budget limitations it was not performed..

- The numerical modelling have shown already from the first excavation step the development of high tangential stresses at the bottom of the cavern walls (lower corners). A spalling effect caused by in situ rock stress problems were observed in the pilot tunnel (Grimstad and Barton 1995).

- The numerical models have shown that there is very little effect of the S (fr) thickness on the overall deformation of the cavern walls. This is mainly due to the large wall heights (49 m) which result in deformation that can not be resisted. Although much larger axial forces are built up in the thicker layer of 20 cm, this does not reduce wall displacements. The S (fr) thickness applied on the walls was 10 and 20 cm for models 1 and 2 respectively.

- An unexpected result is that the thicker arch and wall S (fr) in Model 2 (25 and 20 cm respectively) apparently has a negative effect on bolt loading in the walls. Two possible reasons are apparent: 1) that the thicker arch shotcrete limits stress redistribution to the extent that more load redistribution is thrown on the walls. 2) that the tensile failure of the thicker S (fr) on the walls provides imbalanced forces that are thrown onto the walls at a later stage.

- The deformation in the centre of the crown arch after the nearly fully excavated cavern has been measured by MPBX to be about 24 mm.. The corresponding numerical results after the 3rd numerical excavation stage and after the installation of S (fr) and bolts showed a deformation value of about 34 mm for the same point in the arch.

11 ACKNOWLEDGEMENTS

The authors would like to thank all the colleagues in NGI, CSMRS, NJPC and GSI for their help and contributions in carrying out the research work. The Norwegian Agency for Development (NORAD) is thanked for sponsoring the Indo-Norwegian CSMRS-NGI cooperation programme on tunnelling technology.
The views expressed in the paper are those of the authors .

12 REFERENCES

Barton, N., Lien, R. and Lunde, J., 1974. Engineering classification of rock masses for the design of tunnel support. Rock Mech., 6: 189-236.

Barton, N.,F. Løset, R. Lien and J. Lunde (1980). "Application of the Q-system in design decisions concerning dimensions and appropriate support for underground installations, "Int. Conf. on Sub-surface Space, Rockstore, Stockholm, Sub-surface Space, Vol.2, pp.553-561.

Barton, N., Løset, F., Smallwood, A., Vik, G., Rawlings, C.P., Chryssanthakis, P., Hansteen, H. and Ireland, T. 1992. Geotechnical core characterization for the UK radioactive waste repository design. Proc. ISRM Symp. EUROCK, Chester, UK.

Barton, N., By, T.L. Chryssanthakis, P., Tunbridge, L. Kristiansen, J. Løset, F., Bhasin, R.K., Westerdahl, H. and Vik, G. 1994. Predicted and measured performance of the 62m span Norwegian Olympic Ice Hockey Cavern at Gjøvik. Int. J. Rock Mech. Min. Sci. & Geomech. Abstr. Vol. 31, No. 6, pp. 617-641

Barton, N. and S.C. Bandis (1990). Review of predictive capabilities of JRC-JCS model in engineering practice. International Symposium on Rock Joints. Loen 1990. Proceedings, pp. 603-610.

Bhasin, R Barton, N and Løset, F, 1993. Engineering geological investigations and the application of rock mass classification approach in the construction of Norway's underground Olympic stadium Eng. Geol.,35:93- 101.

Bhasin, R. 1994. Rock mass characterization for large caverns in India and Norway using a new method of recording and presenting engineering geological data. Int. J. Rock Mech. Min. Sci. & Geomech. Abstr. Vol.31, No. 1, 87-91.

Cundall, P.A. (1980). A generalized distinct element program for modelling jointed rock. Report PCAR-1-80, Contract DAJA37-79-C-0548, European Reasearch Office, US Army. Peter Cundall Associates.

Grimstad, E.,N. Barton, R. Lien, J. Lunde, and F. Løset (1986). Classification of Rock Masses with Respect to Tunnel Stability-New Experiences with the Q-system (In Norwegian). Fjellsprengningteknikk, Bergmekanikk, Geoteknikk, p.30.1 - 3.18 Tapir Press, 1986.

Grimstad, E. and Barton, N., 1993. Updating of the Q-System for NMT. Proc. Int. Symp. Modern use of wet mix sprayed concrete for underground support, Fagernes 1993, Norway,: 46-66.

Grimstad, E. and Barton, N., 1995. Rock mass classification and the use of NMT in India. Proc. (under print) Conf. on design and construction of underground structures, 23-25 February 1995, New Delhi, India.

Makurat, A., N. Barton, G. Vik., P. Chryssanthakis and K. Monsen (1990). Jointed rock mass modelling. International Symposium on Rock Joints. Loen 1990. Proceedings, pp. 647-656.

Thakur, V.C. 1992. Geology of Western Himalaya. Physics and chemistry of the earth, Vol. 19 Parts I-VI, Pergamon, England.

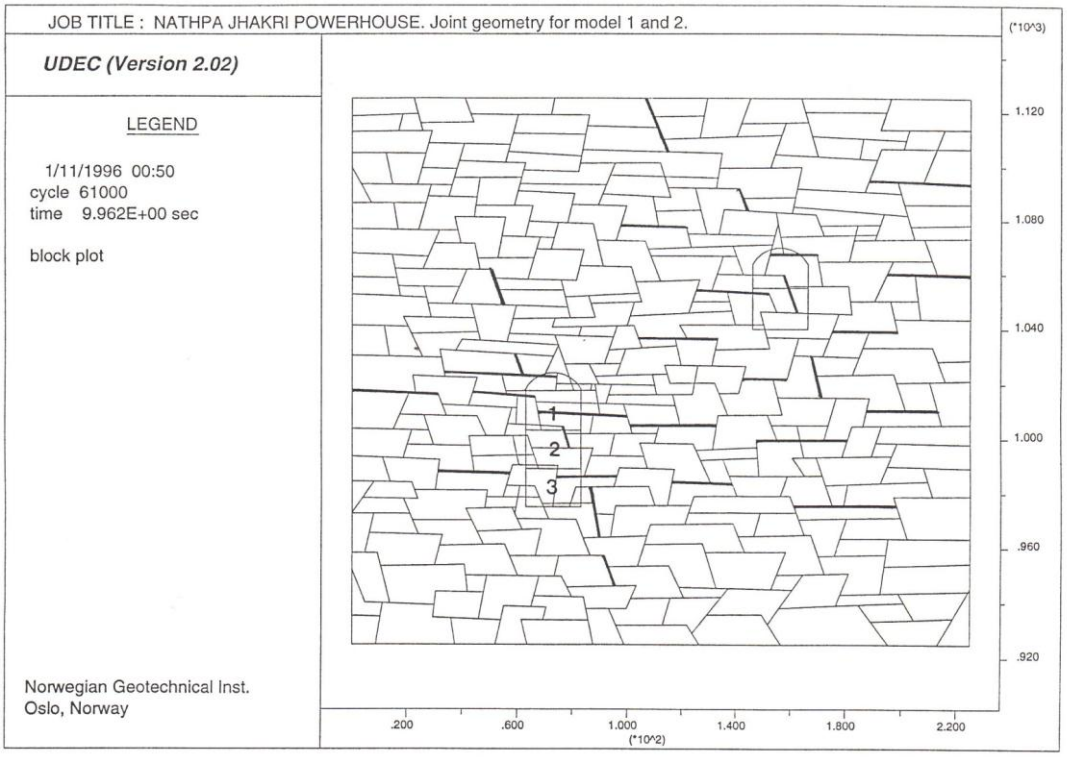

Figure 1: Joint geometry of the powerhouse area. The thicker lines indicate the shear zones in the area. Excavation sequence. The numbers refer to the increasing excavation phase.

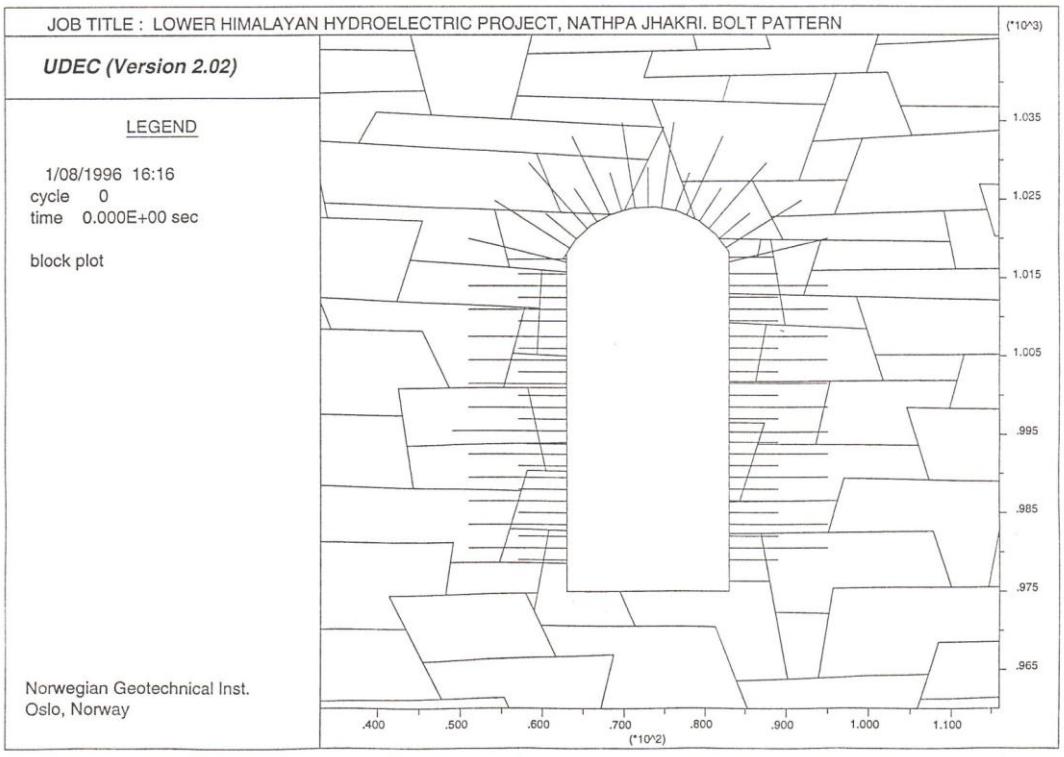

Figure 2: Rock bolt patttern used in models 1 and 2. The bolts had a 32 mm diameter, alternate length of 6 and 12 m and a spacing of 3 m.

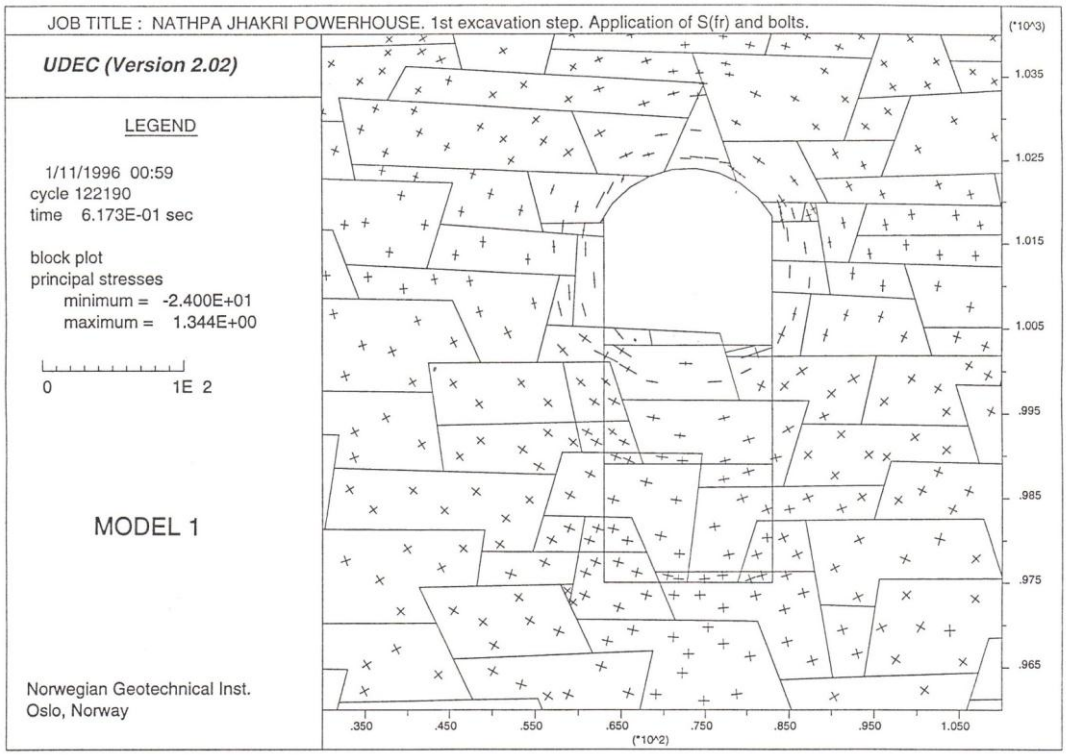

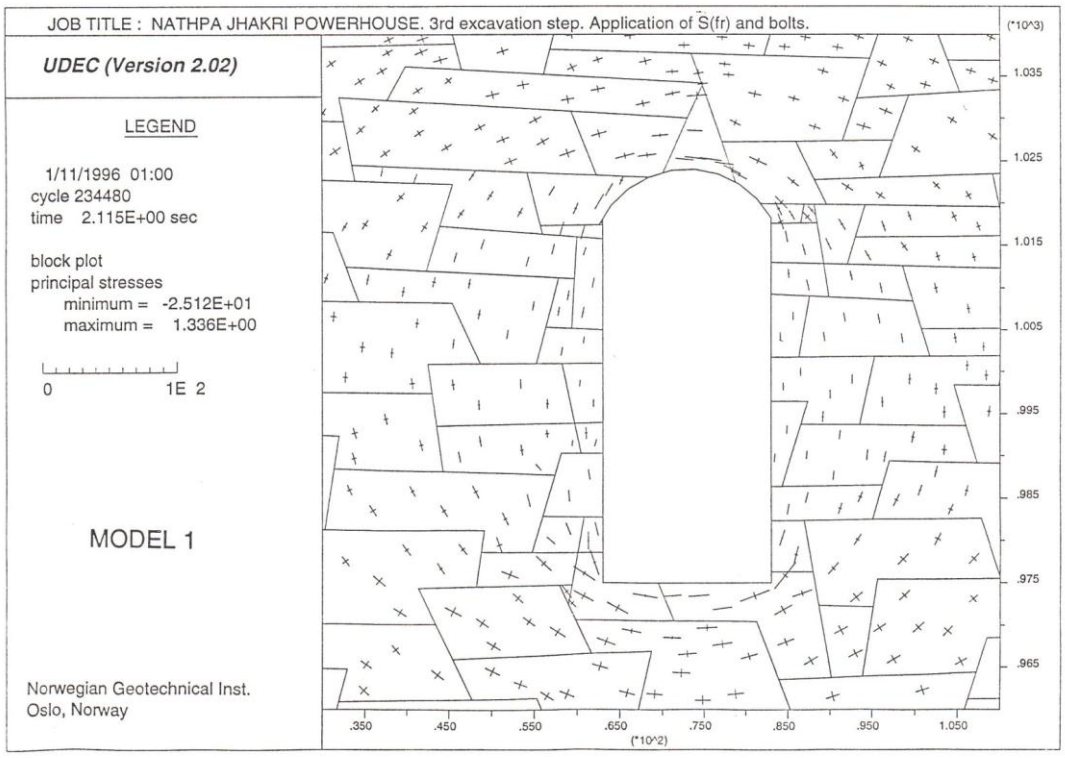

Figure 3: Redistribution of principal stresses between the 1st and the 3rd excavation steps in model 1

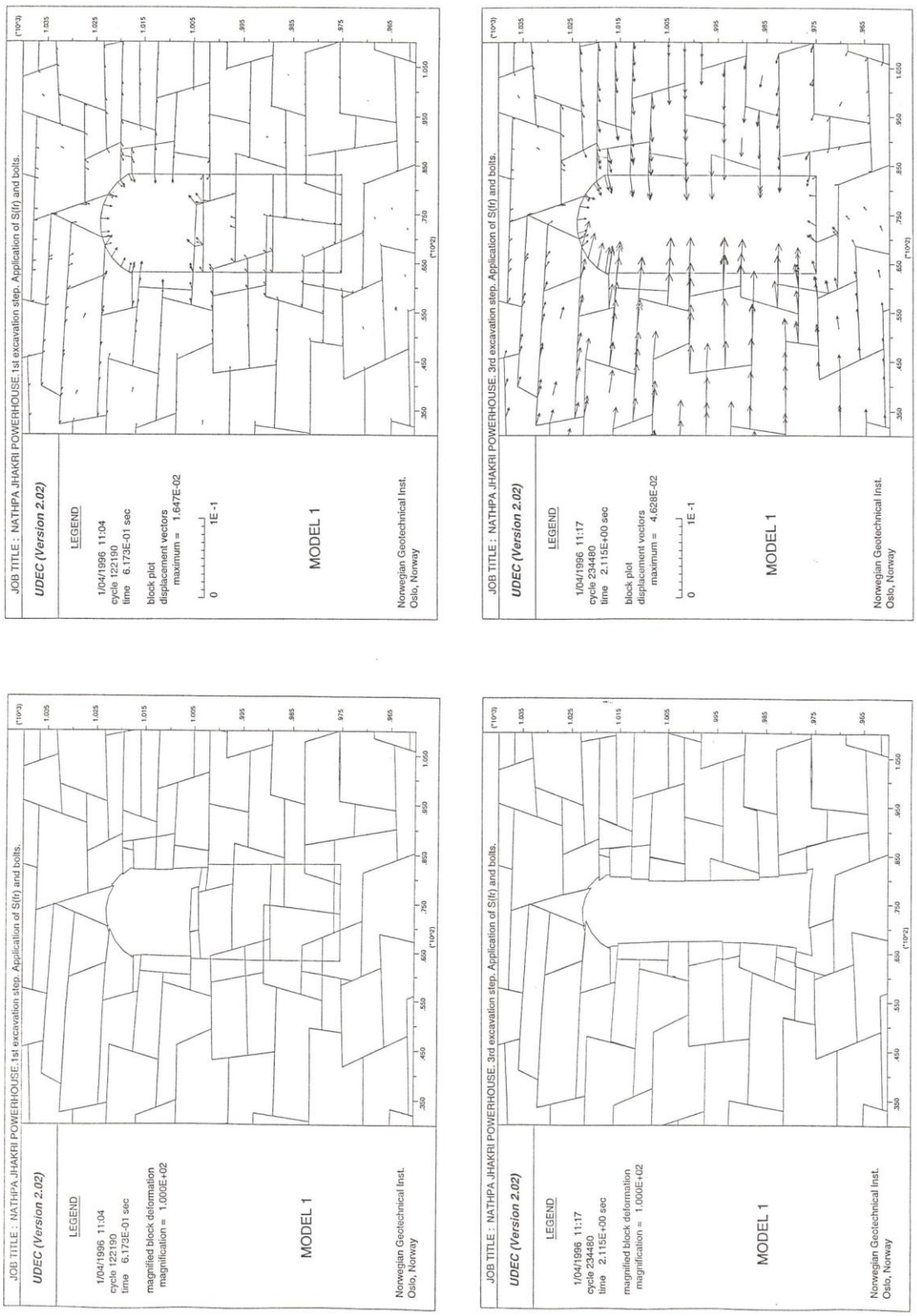

Figure 4: Development of deformation vectors between the 1st and the 3rd excavation step in Model 1. Magnification of the block deformation by 100 times. .

Figure 5: Development of axial fores on the rock bolts after the 3rd excavation step for models 1 and 2.

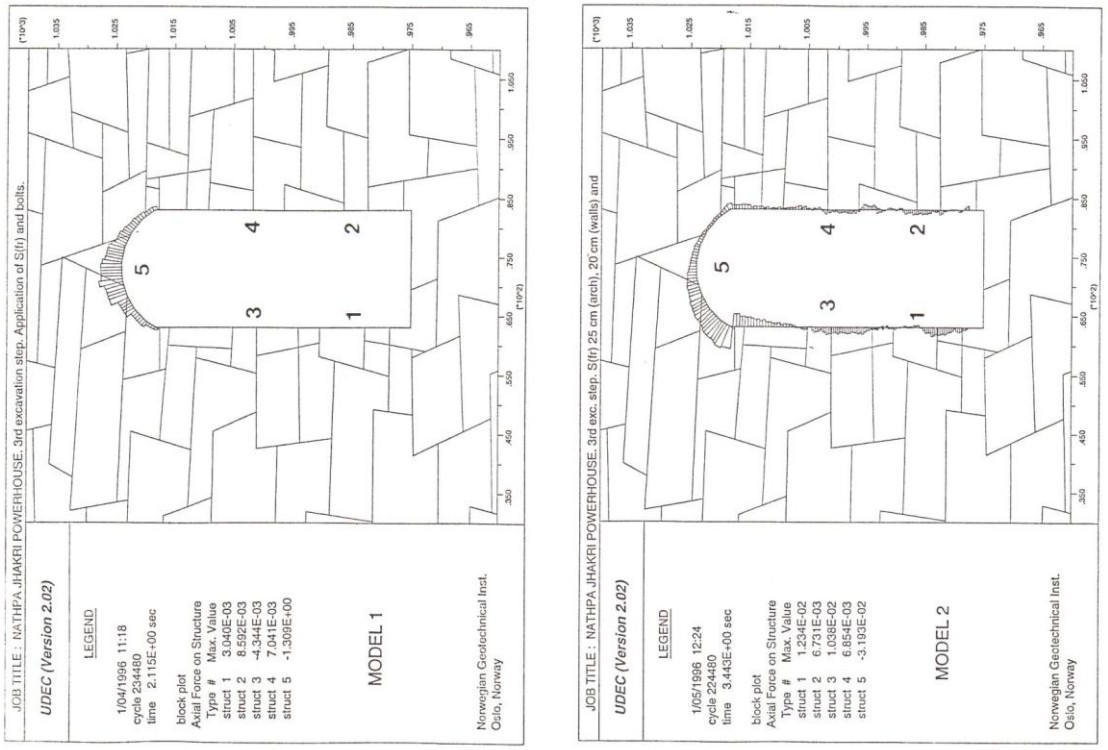

Figure 6: Development of the axial forces in the S (fr) after the 3rd excavation step in models 1 and 2 . The numbers refer on the S (fr) in the plot legend.

Figure 7: Development of the shear forces in the S (fr) after the 3rd excavation step in models 1 and 2 .

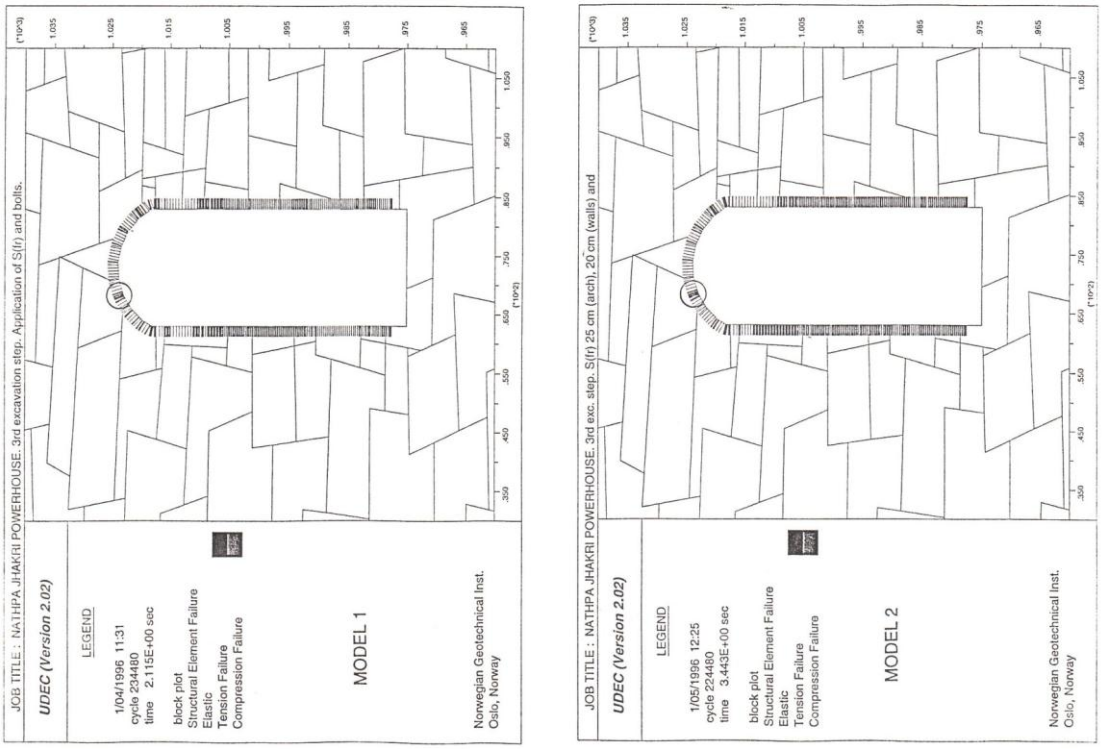

Figure 8: S (fr) failure plot after the 3rd excavation step in model 1 and 2. The area in the circle indicate failure in compression, the thicker lines indicate failure in tension.